Talanta 175 (2017) 535–541

Contents lists available at ScienceDirect

Talanta

journal homepage: www.elsevier.com/locate/talanta

Development of a nanostructured immunosensor for early and *in situ* detection of *Xanthomonas arboricola* in agricultural food production

Matías Regiart[a], Martin Rinaldi-Tosi[b], Pedro R. Aranda[c], Franco A. Bertolino[c], Jhonny Villarroel-Rocha[a], Karim Sapag[a], Germán A. Messina[c], Julio Raba[c], Martín A. Fernández-Baldo[c,*]

[a] *INFAP, Laboratorio de Solidos Porosos, Universidad Nacional de San Luis, CONICET, Ejercito de los Andes 950, D5700BWS San Luis, Argentina*
[b] *CIT-Rio Negro, Laboratorio de Propiedades Nutricionales, Planta Piloto de Alimentos Sociales (PPAS), Centro de Investigación y Transferencia de Rio Negro (CITRN-CONICET), Universidad Nacional de Rio Negro, Argentina*
[c] *INQUISAL, Departamento de Química, Universidad Nacional de San Luis, CONICET, Chacabuco 917, D5700BWS San Luis, Argentina*

ARTICLE INFO

Keywords:
Microfluidic immunosensor
Nanostructured
Agricultural food production
Mesoporous silica
Xanthomonas arboricola

ABSTRACT

We report a microfluidic electrochemical immunosensor for *Xanthomonas arboricola* (XA) determination, based on the covalently immobilization of monoclonal anti-XA antibody (anti-XA) on a previously amino functionalized SBA-15 *in situ* synthesized in the central channel of a glass-poly(dimethylsiloxane) microfluidic immunosensor. The synthetized amino-SBA-15 was characterized by N_2 adsorption-desorption isotherm, scanning electron microscopy and infrared spectroscopy. XA was detected by a direct sandwich immunoassay through an alkaline phosphatase (AP) enzyme-labeled anti-XA conjugate. Later, the substrate p-aminophenyl phosphate was converted to p-aminophenol by AP. The enzymatic product was detected at +100 mV on a sputtered gold electrode. The measured current was directly proportional to the level of XA in walnut trees samples. The linear range was from 5×10^2 to 1×10^4 CFU mL^{-1}. The detection limit was 1.5×10^2 CFU mL^{-1}, and the within- and between-assay coefficients of variation were below 5%. Microfluidic immunosensor is a very promising tool for the early and *in situ* diagnosis of XA in walnuts avoiding serious economic losses.

1. Introduction

Microbial contamination is the main cause of economic losses in fruits and by-products at the post-harvest level. In addition, some microorganisms are toxic, capable of colonizing cultures and accumulating active biomolecules, such as toxins. Toxins pose a major health risk due to the adverse effects of their contact or ingestion. In agricultural-fruit production, the fungi's can produce mycotoxins in edible parts, contaminants and by-products, and thus affect consumer health. The most relevant polluting species belong to the genus *Aspergillus*, *Penicillium*, *Alternaria* and *Fusarium* [1]. However, in the walnut trees (*Juglans regia* L.) as well as in other stone fruit trees, *Xanthomonas arboricola* (XA) pathovars *corylina*, *juglandis*, and *pruni* are the main causative microorganism of brown apical necrosis, blights as well as cankers and pustules on the aerial organs and tissues of the plant. This pathology is responsible of premature drop fruit, damaged fruit and economic losses of over 70% of the production [2,3]. XA is listed as a quarantine organism in the EU phytosanitary legislation (EU Directive 2000/29/CE) and in the European and Mediterranean Plant Protection Organization [4,5].

Plants display different symptoms on leaves, stems and fruits due to plant disease infections. These symptoms are particularly useful for visual observation as a conventional first step for plant disease diagnosis but it fails in detecting the presence of pathogen in early infection stages when plant infections are symptomless [6]. Early detection of plant pathogens plays an important role in plant health monitoring. It allows to manage disease infections and also to minimize the risk of the spread of disease infections to new plants. Many strategies have been widely used for diagnosing plant disease problems including Genomic Analysis [7,8], Flow Cytometry [9] Lateral flow immunoassay [10], PCR [11,12], and Enzyme-linked immunosorbent assays (ELISAs). They usually require no sample clean-up other than filtration and dilution, and allow parallel analysis of multiple samples, being a powerful tool for screening but these laboratory techniques, unfortunately, require highly qualified personnel, tedious assay time, expensive and sophisticated instrumentation. Another disadvantage is that these methods detect the disease in late stages, when the contamination is massive and the fruits are irrecoverable.

During the last years, the development of fast, sensitive, specific

* Corresponding author.
E-mail address: mbaldo@unsl.edu.ar (M.A. Fernández-Baldo).

http://dx.doi.org/10.1016/j.talanta.2017.07.086
Received 6 July 2017; Received in revised form 26 July 2017; Accepted 27 July 2017
Available online 29 July 2017

and, if possible, automated and for *in situ* detection methodologies, have been developed in easy-to-use and economical devices. Electrochemical immunosensors have become more important for the determination of food pollutants [13–15], due to the electrochemical methods provides the required detection limit and fast analysis times. Electrochemical detection allows great versatility, can be easily incorporated into microfluidic sensors, which offer several useful properties including low sample and reagent consumption, short time for analysis, portability, ease of use, high sensitivity and selectivity [16,17].

Glass-poly (dimethylsiloxane) (PDMS) microfluidic sensors are particularly well-suited for integration of electrochemical detection. The glass substrate provides a platform that is thermally stable and amenable to deposition of the electrodes by sputtering [18,19]. PDMS based microfabrication methods are well established and provide an inexpensive method for rapid reproduction of the layer with patterned substrates. So, these sensors offered the best attributes of both substrates and also have the advantages of: low cost, durability, chemical inertness optical transparency, and automation capacity [20–22].

In the last years, different materials have been incorporated into electrochemical immunosensors as immobilization platforms for the specific immunogenic reagents. One the most commonly used solid supports are the different kinds of porous silica materials. These porous silica materials have many benefits, such as the increase of the surface to volume ratio that increases interactions between the immunoreagents and XA, and therefore low the limits of detection [23–25]. We synthetized, functionalized, characterized and used an amino functionalized SBA-15 as immobilization platform for the monoclonal anti-XA antibody (anti-XA). Amino-SBA-15 has an increased surface and uniform porous, compared with the commercial 3-aminopropyl modified controlled pore glass (AP-CPG) normally used as immobilization support [26,27].

In the present work, we developed a glass-PDMS microfluidic electrochemical immunosensor for XA determination, based on the covalently immobilization of monoclonal anti-XA on Amino-SBA-15 synthetized *in situ* in the central channel (CC) of the microfluidic sensor. The mesoporous silica was characterized by N_2 adsorption-desorption isotherm, scanning electron microscopy (SEM) and infrared spectroscopy (FTIR). XA was quantified by a direct sandwich immunoassay measuring through an alkaline phosphatase (AP) enzyme-labeled anti-XA conjugate. Later, the substrate p-aminophenyl phosphate (p-APP) was converted to p-aminophenol (p-AP) by AP. The enzymatic product was oxidized to p-benzoquinonimine (p-BQI) at +100 mV by amperometry on a sputtering gold electrode. The measured current was directly proportional to the level of XA in walnut tree samples. To the best of our knowledge, this is the first microfluidic electrochemical immunosensor, using Amino-SBA-15 as immobilization platform for XA early detection in real samples.

2. Experimental

2.1. Materials and reagents

All reagents used were of analytical reagent grade. Sylgard 184, including PDMS prepolymer and curing agent, and SU-8 photoresist were obtained from Dow Corning (Midland, MI, USA) and Clariant Corporation (Somerville, NJ, USA), respectively. Glutaraldehyde (25% aqueous solution), methanol, ethanol, toluene, tetraethyl orthosilicate (TEOS 98%), and 3-aminopropyl triethoxysilane (3-APTES) were purchased from Merck (Darmstadt, Germany). Bovine serum albumin (BSA), hydrofluoric acid (HF), HCl (37% w/w), Pluronic P123 triblock copolymer (EO20-PO70-EO20), and p-aminophenyl phosphate (pAPP) were purchased from Sigma-Aldrich (St. Louis, MO, USA). ELISA kit and monoclonal anti-XA antibody were purchased from Agdia, Inc. (Elkhart, IN, USA), and it was used according to the manufacturer's instructions. Real walnut samples from Rio Negro valley (Argentina) were used. All the other employed reagents were of analytical grade and were used without further purification. Aqueous solutions were prepared by using purified water from a Milli-Q system.

2.2. Apparatus

Amperometric detection was performed with a BAS LC-4C Electrochemical Detector (Bioanalytical Systems, Inc. West Lafayette, IN, USA). Electrochemical measurements were carried out using an electrochemical cell with three microfabricated gold electrodes. All the potentials in the text were referred to gold. Scanning electron microscope images were taken on a LEO 1450VP (UK), equipped with an Energy Dispersive Spectrometer analyzer, Genesis 2000 (England). Infrared (FTIR) spectroscopic measurements were obtained in a Spectrum 65 FI IR spectrometer Perkin Elmer, in a region from 4000 to 400 cm^{-1}. Textural characterization was carried out by N_2 adsorption-desorption isotherms at 77 K using a manometric adsorption equipment (ASAP 2000, Micromeritics), where the samples were previously degassed at 250 °C for 12 h, up to a residual pressure smaller than 3 Pa.

A syringe pumps system (Baby Bee Syringe Pump, Bioanalytical Systems, Inc. West Lafayette, IN, USA) was used for introducing the solutions in the sensor. All solutions and reagent temperatures were conditioned before the experiment using a Vicking Masson II laboratory water bath (Vicking SRL, Buenos Aires, Argentina). Absorbance was detected by Bio-Rad Benchmark microplate reader (Japan) and Beckman DU 520 general UV/VIS spectrophotometer. All pH measurements were made with an Orion Expandable Ion Analyzer (Orion Research Inc., Cambridge, MA, USA) Model EA 940 equipped with a glass combination electrode (Orion Research Inc).

2.3. Fabrication of the microfluidic immunosensor

Scheme 1 shows a generalized schematic of the design microfluidic immunosensor, whose design consisted of a T-configuration (two inlets, a central channel (CC), and one outlet) with 200-μm-width and 100-μm-height. The microfluidic fabrication involved the following steps: i) Sputtering deposition of the electrodes (Ag/Au) on a glass plate, ii) Fabrication of the PMDS molds with photolithography, iii) Modification of CC through *in situ* polymerization of SBA-15, iv) Sealing of the glass/PDMS, and v) Amino functionalization of SBA-15 and modification with monoclonal anti-XA. The construction of microfluidic immunosensor was carried out according to the procedure proposed by Moraes et al. with the following modifications [28].

A mask designed of self-adhesive vinyl sheet patterned using a blade cutter was employed for the construction of the electrodes. The mask was positioned at the end of the CC and a 20 nm adhesion layer of silver followed by 100 nm of gold, was deposited over a glass plate by sputtering (SPI-Module Sputter Coater, Structure Probe Inc, West Chester, PA). The thickness of the gold electrode was controlled using a Quartz Crystal Thickness Monitor model 12161 (SPI-Module, Structure Probe Inc, West Chester, PA). The vinyl mask was removed after sputtering, leaving the gold tracks on the glass. The geometric areas of the electrodes are 1.0 mm^2 for the working electrode and 2.0 mm^2 for counter and reference electrodes.

The microchannels in the PDMS were cast by photolithography [29]. The design of the channels in the negative mask was generated by a computer drawing program. The replication master was patterned with a SU-8 photoresist layer over a silicon wafer using a spin coater at 2000 rpm for 30 s, and baked at 65 °C for 2 min and 95 °C for 6 min. Then, the coated sheet was exposed to UV lamp through a negative mask design containing the desired channel. After that, the unexposed photoresist was removed, the Sylgard curing agent and PDMS prepolymer were mixed in a 1:10 weight ratio and the mixture was placed on the replication master and degassed for 30 min to eliminate air bubbles. The polymer curing process was carried out in a hot plate at

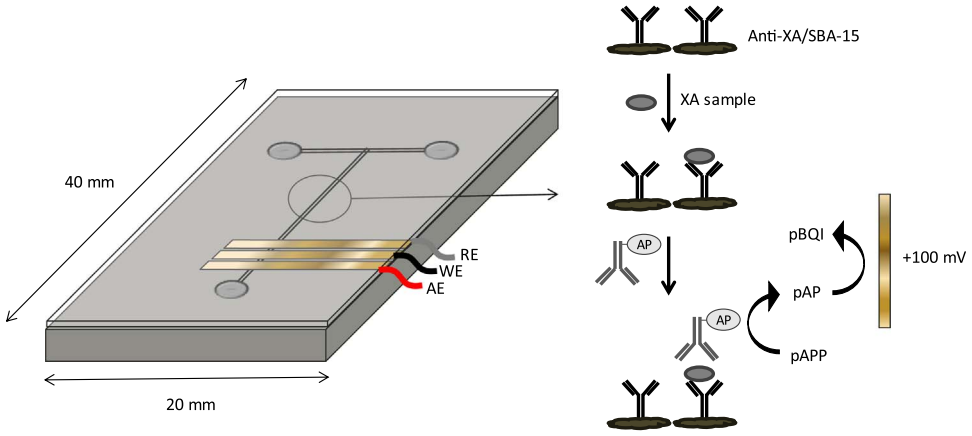

Scheme 1. Analytical procedure for XA determination in walnut plant samples.

Table 1
Sequence required for XA determination in walnut plant samples.

Sequence	Condition[a]	Time (min)
Desorption buffer	0.1 mol L^{-1} glycine-HCl pH 2.00	5
Washing buffer	0.01 mol L^{-1} PBS pH 7.00	2
Blocking solution	1% BSA in 0.01 mol L^{-1} PBS pH 7.00	5
Washing buffer	0.01 mol L^{-1} PBS pH 7.00	2
Walnut plant sample	Diluted 10-fold with 0.01 mol L^{-1} PBS pH 7.00	5
Washing buffer	0.01 mol L^{-1} PBS pH 7.00	2
Enzyme conjugate	AP-conjugated anti-XA 1:500 with 0.01 mol L^{-1} PBS pH 7.00	5
Washing buffer	0.01 mol L^{-1} PBS pH 7.00	2
Substrate	2 mmol L^{-1} p-APP in DEA buffer, pH 9.50	1
Signal analysis	LC-4C amperometric detector, +100 mV	1

[a] All solutions employed were injected using syringe pumps at 4 μL min^{-1} flow rate.

65 °C for 1 h, and was followed by peeling off the PDMS layers. The external access to the microfluidic sensor was obtained by drilling holes in the PDMS. After the CC modification with SBA-15, the glass plate and PDMS were placed in oxygen plasma for 1 min, and were contacted immediately for a strong seal.

2.4. Synthesis and modification of SBA-15 by in situ polymerization

A glass pretreatment was carry out in order to increase the roughness and bonding surface. Firstly, CC was washed several times with methanol and double distilled water. In a second step, it was treated with 0.1 mol L^{-1} HF at 50 °C for 2 h, followed by a washing step with methanol and double distilled water. Then, CC was put in contact with 5 mol L^{-1} KOH at 95 °C for 5 h, and then washed with doubly distilled water until pH 7.00.

SBA-15 was synthesized using the procedure reported by Barrera et al. [30]. The molar ratio used for the preparation of the SBA-15 were: 0.017P123:1TEOS:6HCl:140H_2O. Before to start the SBA-15 synthesis, the glass treated was placed in the flask where the reaction mixture will occur. First, P123 was dissolved in an aqueous solution of 2 mol L^{-1} HCl and kept under stirring at 45 °C for 3 h. Then, the TEOS was added drop-wise to this solution and kept under vigorous stirring for 4 h at the same temperature. Afterwards, this mixture was aged at 40 °C for 20 h without stirring. Subsequently, the temperature was raised to 80 °C and maintained at this value for 48 h. After, the glass treated was put out of the final reaction mixture and immersed in ethanol (in order to remove the P123 surfactant by extraction) for 96 h, and later this glass was dried at room temperature. Finally, the solids of the final mixture were filtrated, washed with abundant deionized water until reaching a conductivity value smaller than 10 μS cm^{-1}, dried at 80 °C for 12 h and calcined at 500 °C for 6 h.

Amino functionalization was prepared according to the procedure described above, with some modifications [31]. Firstly, 1 mL of APTES (50 mmol L^{-1}) was flowed through the CC under N_2 flowing and vigorous stirring. Then, the mixture was refluxed at 80 °C for 6 h. Finally, the CC was washed with toluene followed by ethanol, and dried at 60 °C for 12 h.

2.5. Immobilization of the monoclonal anti-XA in the amino functionalized SBA-15

To perform the monoclonal anti-XA antibodies immobilization process, 1 mL of 5% w/w glutaraldehyde solution (0.10 mol L^{-1} sodium phosphate buffer, pH 8.00) was introduced to the CC for 2 h

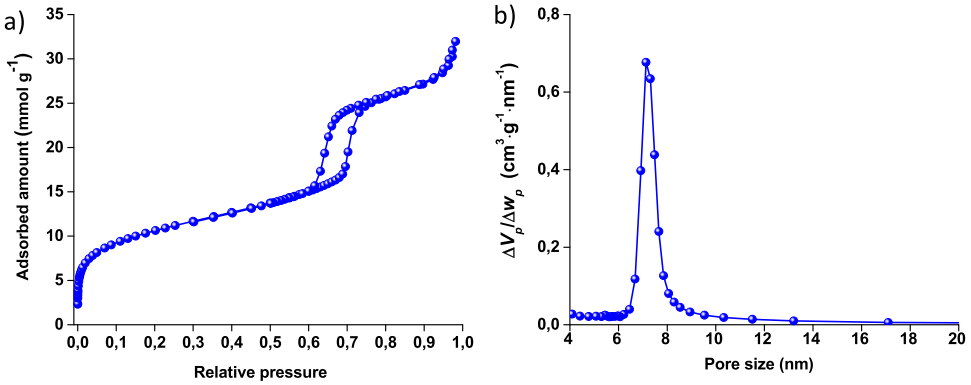

Fig. 1. (a) N_2 adsorption–desorption isotherms at 77 K, and (b) Mesopore size distribution of SBA-15.

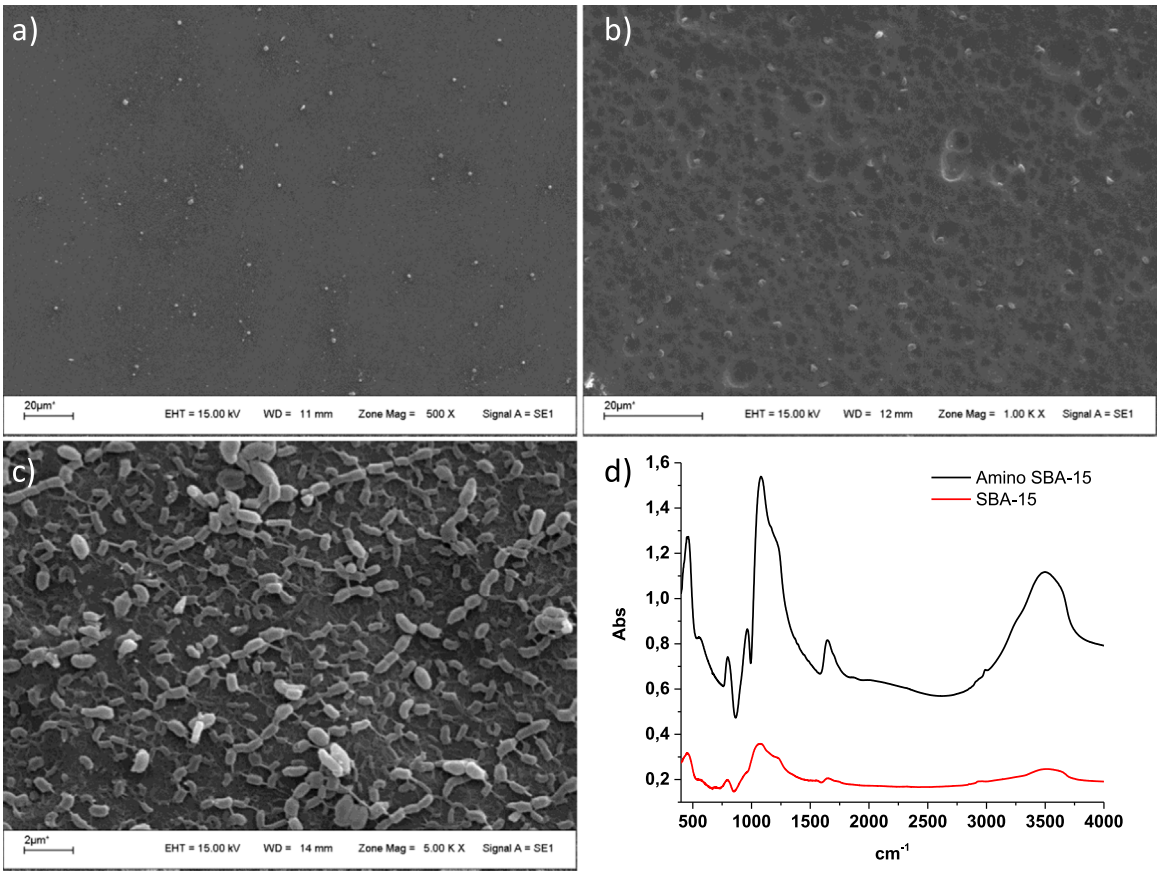

Fig. 2. SBA-15 characterization. (a) SEM micrograph of glass without chemical treatment, (b) SEM micrograph of glass with chemical treatment, (c) SEM micrograph of glass modified with SBA-15, and (d) FTIR measurements of SBA-15 and amino SBA-15.

at room temperature. After three washes with 0.01 mol L^{-1} phosphate buffer saline (PBS) pH 7.00, 250 µL of antibody preparation (dilution 1:200 in 0.01 mol L^{-1} PBS pH 7.00) was coupled to the residual aldehyde groups by cycle flow for 12 h at 4 °C. The immobilized antibody preparation was finally washed three times with PBS (0.01 mol L^{-1} pH 7.00) and stored in the same buffer at 4 °C. Anti-XA/SBA-15 was perfectly stable for at least 1 month.

2.6. Sample preparation

The walnut blight bacteria over winter is in the outer bud scales. Within the dormant bud, the inner leaf tissue and flowers are pathogen free. As the shoot grows through the infected outer bud scales, bacterial have the opportunity to move and infect developing leaves, shoots and flowers. Infection occurs when rainfall, heavy dew or otherwise wet conditions transport blight bacteria to developing tissue. The probability of infection depends upon how much pathogen exists on individual buds and environmental conditions favoring bacterial spread and infection [32].

In this way, the better option is to control the pathogen in the winter over the outer bud scales, so if the result is positive a product can be used to protect the walnut tree. Good quality spray copper products are currently the most effective choice for controlling walnut blight. This places a protective layer of bactericide on leaf tissue. If bacteria are splashed from the outer bud scales to developing shoots and flowers, the bactericide barrier prevents infection and subsequent blight lesions.

Firstly, the outer bud scales were washed with double distilled sterile water to obtain the bacterial sample. The extract was filtered through a Whatman #1 filter and collected. Then was centrifuged at 5000 rpm. Finally, the pellet was resuspended in 0.01 mol L^{-1} PBS pH 7.00 and stored in the same buffer at 4 °C.

2.7. Analytical procedure for XA quantification

The procedure for the XA determination involves the following steps (Table 1). The carrier buffer was 0.01 mol L^{-1} PBS pH 7.00. The following solutions were injected at a flow rate of 4 µL min^{-1}. Firstly, the microfluidic immunosensor was exposed to a desorption buffer (0.1 mol L^{-1} glycine-HCl pH 2.00) for 5 min and then was rinsed with 0.01 mol L^{-1} PBS pH 7.00 for 2 min. This treatment was carried out in order to desorb the immune-complex and start with a new analysis. Unspecific binding was blocked with 1% BSA in 0.01 mol L^{-1} PBS pH 7.00 by a 5 min treatment at room temperature and then was rinsed with 0.01 mol L^{-1} PBS pH 7.00 for 2 min.

After that, the walnut plant sample (diluted 10-fold with 0.01 mol L^{-1} PBS pH 7.00), was injected into the PBS carrier stream for 5 min. Once the XA was recognized and captured by monoclonal anti-XA immobilized on the SBA-15, the microfluidic immunosensor was washed with 0.01 mol L^{-1} PBS pH 7.00 for 2 min to remove excess of sample. Later, the AP-conjugated anti-XA (diluted 1:500 with 0.01 mol L^{-1} PBS pH 7.00) was added for 5 min followed by a washing procedure with 0.01 mol L^{-1} PBS pH 7.00 for 2 min. Finally, the substrate solution (2 mmol L^{-1} pAPP in DEA buffer (0.1 mol L^{-1} diethanolamine, 0.05 mol L^{-1} KCl, 1 mmol L^{-1} $MgCl_2$, pH 9.50)) was pumped and the enzymatic product (p-AP) was oxidized to p-BQI at +100 mV (Scheme 1). The sensor could be used with no significant loss of sensitivity for 15 days, whereas its useful lifetime was one month with a sensitivity decrease of 15%. When not in use the microfluidic immunosensor was storage in 0.01 mol L^{-1} PBS pH 7.00 at 4 °C.

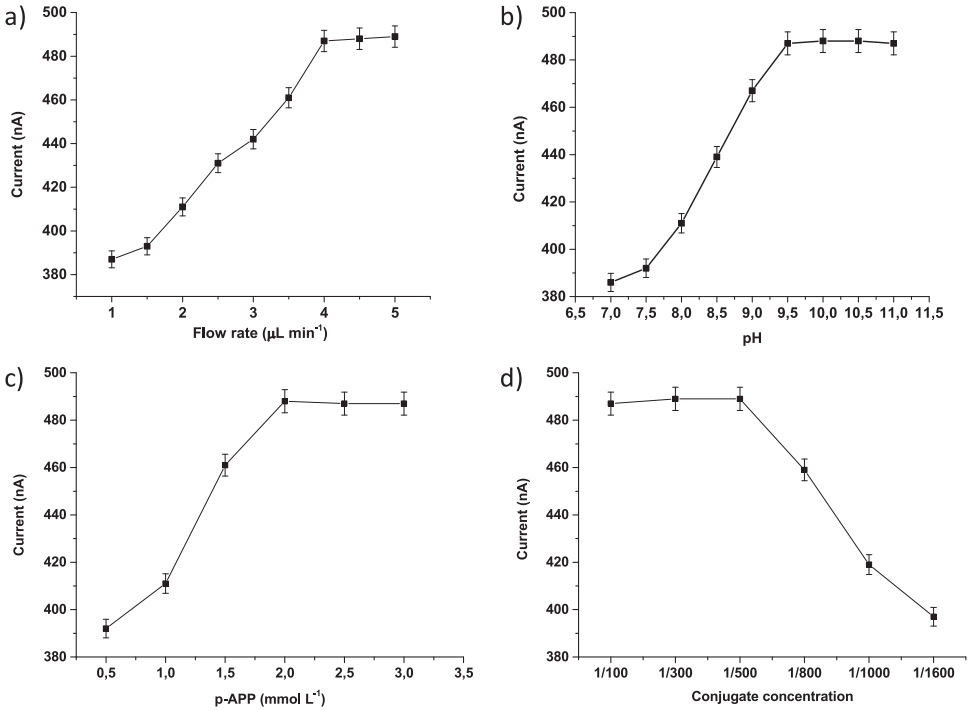

Fig. 3. Variables optimization. (a) Flow rate effect, (b) pH, (c) Concentration of p-APP, and (d) Conjugate concentration, using a XA control of 5×10^3 CFU mL^{-1}.

3. Results and discussion

3.1. Characterization of AMS

The specific surface area (SBET) of materials under study was estimated by the Brunauer, Emmet and Teller (BET) method [33], using the adsorption data in the range of relative pressures from 0.05 to 0.18. The total pore volume (VTP) was determinated by the Gurvich's rule at a relative pressure of 0.98 [34]. The micropore volume (VμP) and the primary mesopore volume (VPMP) were calculated by the αS-plot method using the LiChrospher Si-1000 macroporous silica gel [35] as the reference adsorbent. The mesopore size distribution (PSD) of the SBA-15 was obtained by the VBS macroscopic method [36] using the desorption branch data. In Fig. 1(a) N_2 adsorption–desorption isotherm at 77 K of the SBA-15 is shown. This material presents a Type IV isotherm with a hysteresis loop H1 type which is typical of mesoporous materials with well-defined mesopore sizes. The textural properties of SBA-15, obtained from adsorption data, were SBET: 860 $m^2 g^{-1}$, VμP: 0.06 $cm^3 g^{-1}$, VPMP: 0.53 $cm^3 g^{-1}$ and VTP: 1.10 $cm^3 g^{-1}$. Fig. 1(b) shows a narrow pore size distribution of SBA-15 with a mesopore width around of 7.1 nm.

SBA-15 characterization can be seen in the Fig. 2. (a) SEM micrograph of glass without chemical treatment, (b) SEM micrograph of glass with chemical treatment, (c) SEM micrograph of glass modified with SBA-15. In the FTIR measurements, it can be observed the changed between the SBA-15 and Amino-SBA-15 in the peaks Si-OH (965), C-N, Si-O-Si, Si-CH_2-R (1220), -OH (3500), H-O-H (1645), N-H (690), NH_3^+ (1555), Si-O-Si (800), Si-O-Si (460) (Fig. 2(c)).

3.2. Optimization of experimental variables

Relevant studies of experimental variables that affect the performance of microfluidic immunosensor for XA determination in walnut plant samples were done. For this purpose, an XA control of 5×10^3 CFU mL^{-1} was employed.

One of the most important parameters to consider in the optimization procedure of the microfluidic sensor is the flow rate. The flow rates of the sample and reagents have effect on the reaction efficiencies of the antigen–antibody complex. Optimal flow rate was determined by employing different flow rates and evaluating the current generated during the immune reaction. As shown in Fig. 3(a), flow rates from 1 to 4 μL min^{-1} had little effect on the antigen-antibody reaction. Conversely, when the flow rate exceeded 4 μL min^{-1}, the signal was dramatically reduced. Taking into account the magnitude of the current response and analysis time for each sample, 4 μL min^{-1} was chosen for samples, reagents and washing buffer injection.

Another relevant parameter is the pH. The rate of enzymatic response under flow conditions was studied in the pH range from 7 to 11 and reached a maximum value of activity at pH 9.50. The pH value used was 9.50 in DEA buffer (Fig. 3(b)). As can be seen in Fig. 3(c), the effect of varying p-APP concentration from 0.5 to 3 mmol L^{-1} on the electrochemical immunosensor response was evaluated. The optimum p-APP concentration was 2 mmol L^{-1}.

Another parameter studied was the enzyme conjugate concentration. This factor was evaluated using anti-XA AP-conjugated in 1:100, 1:300, 1:500, 1:800, 1:1000 and 1:1600. The rate of response increased with concentrated solutions until 1:500, where can be observed an increase in the sensitivity, later insignificant differences can be noted when the solutions of 1:300 and 1:100 were used. So, an AP-conjugated

Table 2
Comparison of XA concentration in walnut plant samples by our microfluidic electrochemical immunosensor and a commercial ELISA.

Samples[a]	XA (CFU mL^{-1})	
	MEI[b]	ELISA
WS 1	150 ± 12[c]	–
WS 2	500 ± 18	–
WS 3	1000 ± 34	–
WS 4	2000 ± 58	1889 ± 65
WS 5	5000 ± 76	5132 ± 96
WS 6	10,000 ± 111	9899 ± 134

[a] Walnut plant samples.
[b] Microfluidic electrochemical immunosensor.
[c] Mean of three determinations ± S.D.

Table 3
Comparison with other works using different techniques for XA determination.

Techniques	Samples	LD(CFU mL^{-1})	Analysis time (min)	Reference
Pan-Genomic Analysis	Barley, Tabacum	10^1	–	[7]
Loop-mediated isothermal amplification assay	Strawberry	10^2	20	[8]
Flow Cytometry	Cabbage	10^3	32	[9]
Lateral flow immunoassay	Prunus, Juglans regia	10^4	15	[10]
Real-time quantitative polymerase chain reaction	Sugarcane	10^2	–	[12]
Microfluidic electrochemical immunosensor	Walnut	10^2	30	[This work]

concentration of 1:500 was used (Fig. 3(d)). As seen for quantification of XA, small reactive volumes are required; this point is very important because the cost of reagents can be very expensive. Therefore, it has always been an aim to reduce reagents volume and increase sensitivity in all biological assays.

3.3. Analytical performance

Linearity and range of the developed microfluidic immunosensor were studied by analyzing several concentration solutions containing 1 × 10^2 to 5 × 10^4 CFU mL^{-1}. A linear relation was observed between the concentration range from 5 × 10^2 to 1 × 10^4 CFU mL^{-1}. The calibration curve was described according to the following equation: ΔI (nA) = 150.73 + 7.18 × 10^{-2} [XA] (CFU mL^{-1}) with a correlation coefficient of 0.984, where ΔI is the difference between the blank and sample current. For microfluidic immunosensor and commercial ELISA, the detection limits were 1.5 × 10^2 and 1.8 × 10^3 CFU mL^{-1}, respectively.

The coefficient of variation (VC) for the determination of 5 × 10^3 CFU mL^{-1} XA was 4.5% (n = 5). The within-assay precision was tested with five measurements in the same run for each control. These series of five measurements were repeated for three consecutive days to estimate between-assay precision. The VC within-assay values were below 4.7% and the between assay values below 5.3%. Moreover, the microfluidic immunosensor was compared with a commercial ELISA for the XA quantification in six walnut plant samples under the conditions previously described. The results demonstrated that both methods were statistically equal at a confidence level of 95% (Table 2).

Table 3 shows previously published articles for XA determination in several plant samples using different methods. Our analytical method has significant advantages over the previously reported. The present method is a microfluidic electrochemical immunosensor that use amperometry as detection technique, which offers sensitive determinations in short analysis time, with a low consumption of reagents and samples. Furthermore, the achieved detection limit is lower than that obtained by the methods recently reported. In addition, our system uses the amino functionalized SBA-15 platform for immobilizing the monoclonal anti-XA antibodies, which provides specificity. Finally, our immunosensor has the potential to answer the growing needs for analytical tools that fulfill requirements such as low cost, sensitivity and short analysis time.

4. Conclusions

This article described the development of a microfluidic electrochemical immunosensor for the quantitative detection of XA in walnut plant samples. Our analytical method is based on the covalently immobilization of monoclonal anti-XA antibodies on amino functionalized SBA-15 synthetized *in situ* in the central channel of a microfluidic immunosensor. The assay time employed (30 min) was shorter than the reported for ELISA test kit (90 min) frequently used. The microfluidic immunosensor offered several attractive advantages like high stability, high selectivity and sensitivity. In conclusion, our method is a very promising tool for the early and *in situ* diagnosis of XA in walnut plants avoiding serious economic losses.

Acknowledgements

The authors wish to thank the financial support from Universidad Nacional de San Luis (PROICO 22/Q241), Instituto de Química de San Luis (INQUISAL), Instituto de Física Aplicada (INFAP), Consejo Nacional de Investigaciones Científicas y Técnicas (CONICET) (PIP 11220150100004CO) and the Agencia Nacional de Promoción Científica y Tecnológica (PICT – 2014-0375).

References

[1] M. Khater, A. Escosura-Muñiz, A. Merkoçi, Biosensors for plant pathogen detection, Biosens. Bioelectron. 93 (2016) 72–86.
[2] J.R. Lamichhane, L. Varvaro, Xanthomonas arboricola disease of hazelnut: current status and future perspectives for its management, Plant Pathol. 63 (2014) 243–254.
[3] A. Akkopru, Determination of bacterial disease on stone fruits grown in Lake Van Basin, East Anatolia of Turkey, Acta Hortic. 1149 (2016) 15–20.
[4] Diagnosis protocols for regulated pests Xanthomonas arboricola pv. Corylina, EPPO Bull. 179, 2004, pp. 179–181.
[5] Diagnostics Xanthomonas arboricola pv. pruni, EPPO Bull. 36, 2006, pp. 129–133.
[6] J.R. Lamichhane, Xanthomonas arboricola diseases of stone fruit, almond, and walnut trees: progress toward understanding and management, Plant Dis. 98 (2014) 1600–1610.
[7] J. Garita-Cambronero, A. Palacio-Bielsa, M.M. López, J. Cubero, Pan-genomic analysis permits differentiation of virulent and non-virulent strains of Xanthomonas arboricola that cohabit prunus spp. and elucidate bacterial virulence factors, Front. Microbiol. 8 (2017) 1–17.
[8] M. Gétaz, A. Bühlmann, P.H.H. Schneeberger, C. Van Malderghem, B. Duffy, M. Maes, J.F. Pothier, B. Cottyn, A diagnostic tool for improved detection of Xanthomonas fragariae using a rapid and highly specific LAMP assay designed with comparative genomics, Plant Pathol. (2017) 12665–12674.
[9] G. Chitarra, C.J. Langerak, J.H.W. Bergervoet, R.W. Van den Bulk, Detection of the plant pathogenic bacterium Xanthomonas campestris pv. campestris in seed extracts of brassica sp. applying fluorescent antibodies and flow cytometry, Cytometry 47 (2002) 118–126.
[10] P. Lopez-Soriano, P. Noguera, M.T. Gorris, R. Puchades, A. Maquieira, E. Marco-Noales, M.M. Lopez, Lateral flow immunoassay for on-site detection of Xanthomonas arboricola pv. pruni in symptomatic field samples, PLoS One 12 (2017) 1–13.
[11] S.Y. Park, Y.S. Lee, Y.J. Koh, J.S. Hur, J.S. Jung, Detection of Xanthomonas arboricola pv. pruni by PCR using primers based on DNA sequences related to the hrp genes, J. Microbiol. 48 (2010) 554–558.
[12] F.F. Garces, A. Gutierrez, J.W. Hoy, Detection and quantification of Xanthomonas albilineans by qPCR and potential characterization of sugarcane resistance to leaf scald, Plant Dis. 98 (2014) 121–126.
[13] G. Vásquez, A. Rey, C. Rivera, C. Iregui, J. Orozco, Amperometric biosensor based on a single antibody of dual function for rapid detection of Streptococcus agalactiae, Biosens. Bioelectron. 87 (2017) 453–458.
[14] A. Güner, E. Çevik, M. Şenel, L. Alpsoy, An electrochemical immunosensor for sensitive detection of Escherichia coli O157:H7 by using chitosan, MWCNT, polypyrrole with gold nanoparticles hybrid sensing platform, Food Chem. 229 (2017) 358–365.
[15] X. Zhang, Y. Jiang, C. Huang, J. Shen, X. Dong, G. Chen, W. Zhang, Functionalized nanocomposites with the optimal graphene oxide/Au ratio for amplified immunoassay of E. coli to estimate quality deterioration in dairy product, Biosens. Bioelectron. 89 (2016) 913–918.
[16] M. Regiart, M.A. Fernández-Baldo, V.G. Spotorno, F.A. Bertolino, J. Raba, Ultra sensitive microfluidic immunosensor for determination of clenbuterol in bovine hair samples using electrodeposited gold nanoparticles and magnetic micro particles as bio-affinity platform, Biosens. Bioelectron. 41 (2013) 211–217.
[17] F. Tan, P.H.M. Leung, Z.B. Liu, Y. Zhang, L. Xiao, W. Ye, X. Zhang, L. Yi, M. Yang, A PDMS microfluidic impedance immunosensor for E. coli O157:H7 and Staphylococcus aureus detection via antibody-immobilized nanoporous membrane, Sens. Actuators B Chem. 159 (2011) 328–335.
[18] A. Hatamie, A. Echresh, B. Zargar, O. Nur, M. Willander, Fabrication and characterization of highly-ordered zinc oxide nanorods on gold/glass electrode, and its application as a voltammetric sensor, Electrochim. Acta 174 (2015) 1261–1267.

[19] H. Zhu, Y. Xu, A. Liu, N. Kong, F. Shan, W. Yang, C.J. Barrow, J. Liu, Graphene nanodots-encaged porous gold electrode fabricated via ion beam sputtering deposition for electrochemical analysis of heavy metal ions, Sensor, Actuators B Chem. 206 (2015) 592–600.
[20] J. Casanova-Moreno, J. To, C.W.T. Yang, R.F.B. Turner, D. Bizzotto, K.C. Cheung, Fabricating devices with improved adhesion between PDMS and gold-patterned glass, Sens. Actuators B Chem. 246 (2017) 904–909.
[21] N. Li, X. Hai, X. Yu, F. Dang, Carbohydrate analysis on hybrid poly(dimethylsiloxane)/glass chips dynamically coated with ionic complementary peptide, J. Chromatogr. A 1481 (2017) 152–157.
[22] F. Costantini, C. Sberna, G. Petrucci, M. Reverberi, F. Domenici, C. Fanelli, C. Manetti, G. de Cesare, M. DeRosa, A. Nascetti, Aptamer-based sandwich assay for on chip detection of Ochratoxin A by an array of amorphous silicon photosensors, Sens. Actuators B Chem. 230 (2016) 31–39.
[23] P. Wang, M. Li, F. Pei, Y. Li, Q. Liu, Y. Dong, Q. Chu, H. Zhu, An ultrasensitive sandwich-type electrochemical immunosensor based on the signal amplification system of double-deck gold film and thionine unite with platinum nanowire inlaid globular SBA-15 microsphere, Biosens. Bioelectron. 91 (2017) 424–430.
[24] X. Li, Y. Li, R. Feng, D. Wu, Y. Zhang, H. Li, B. Du, Q. Wei, Ultrasensitive electrochemiluminescence immunosensor based on Ru(bpy)32+ and Ag nanoparticles doped SBA-15 for detection of cancer antigen 15-3, Sens. Actuators B Chem. 188 (2013) 462–468.
[25] R. Li, H. Yu, Y. Li, R. Feng, X. Li, H. Li, Q. Wei, B. Du, Ultrasensitive label-free immunoassay for diethylstilbestrol based on Au nanoparticles on mesoporous silica and amino-functionalized graphene, Anal. Methods 5 (2013) 5534–5540.
[26] M.A. Seia, S.V. Pereira, C.A. Fontán, I.E. De Vito, G.A. Messina, J. Raba, Laser-induced fluorescence integrated in a microfluidic immunosensor for quantification of human serum IgG antibodies to Helicobacter pylori, Sens. Actuators B Chem. 168 (2012) 297–302.
[27] S.V. Pereira, J. Raba, G.A. Messina, IgG anti-gliadin determination with an immunological microfluidic system applied to the automated diagnostic of the celiac disease, Anal. Bioanal. Chem. 396 (2010) 2921–2927.
[28] F.C. Moraes, R.S. Lima, T.P. Segato, I. Cesarino, J.L. Melendez Cetino, S.A. Spinola Machado, F. Gomez, E. Carrilho, Glass/PDMS hybrid microfluidic device integrating vertically aligned SWCNTs to ultrasensitive electrochemical determinations, Lab Chip 12 (2012) 1959–1962.
[29] D.C. Duffy, J. Cooper McDonald, O.J.A. Schueller, G.M. Whitesides, Rapid prototyping of microfluidic systems in poly(dimethylsiloxane), Anal. Chem. 70 (1998) 4974–4984.
[30] D. Barrera, J. Villarroel-Rocha, K. Sapag, Non-hydrothermal synthesis of cylindrical mesoporous materials: influence of the surfactant/silica molar ratio, Adsorpt. Sci. Technol. 29 (2011) 975–988.
[31] J. Sun, D. Ma, H. Zhang, X. Liu, X. Han, X. Bao, G. Weinberg, N. Pfänder, D. Su, Toward monodispersed silver nanoparticles with unusual thermal stability, J. Am. Chem. Soc. 128 (2006) 15756–15764.
[32] Richard P. Buchner, 2012, Walnut Blight Management. ⟨http://cebutte.ucanr.edu/newsletters/Walnut_Notes42284.pdf⟩.
[33] S. Brunauer, P.H. Emmett, E. Teller, Adsorption of gasses in multimolecular layers, J. Am. Chem. Soc. 60 (1938) 309–319.
[34] F. Rouquerol, J. Rouquerol, K.S.W. Sing, P. Llewellyn, G. Maurin, Adsorption by Powders and Porous Solids: Principles, Methodology and Applications, Academic Press, San Diego, 2014.
[35] M. Jaroniec, M. Kruk, J. Olivier, Standard nitrogen adsorption data for characterization of nanoporous silicas, Langmuir 15 (1999) 5410–5413.
[36] J. Villarroel-Rocha, D. Barrera, K. Sapag, Improvement in the pore size distribution for ordered mesoporous materials with cylindrical and spherical pores using the Kelvin equation, Top. Catal. 54 (2011) 121–134.